Optogenetics

International Edition: DOI: 10.1002/anie.201911025
German Edition: DOI: 10.1002/ange.201911025

Near-Infrared Optogenetic Genome Engineering Based on Photon-Upconversion Hydrogels

Yoichi Sasaki, Mio Oshikawa, Pankaj Bharmoria, Hironori Kouno, Akiko Hayashi-Takagi, Moritoshi Sato, Itsuki Ajioka, Nobuhiro Yanai,* and Nobuo Kimizuka**

Abstract: *Photon upconversion (UC) from near-infrared (NIR) light to visible light has enabled optogenetic manipulations in deep tissues. However, materials for NIR optogenetics have been limited to inorganic UC nanoparticles. Herein, NIR-light-triggered optogenetics using biocompatible, organic TTA-UC hydrogels is reported. To achieve triplet sensitization even in highly viscous hydrogel matrices, a NIR-absorbing complex is covalently linked with energy-pooling acceptor chromophores, which significantly elongates the donor triplet lifetime. The donor and acceptor are solubilized in hydrogels formed from biocompatible Pluronic F127 micelles, and heat treatment endows the excited triplets in the hydrogel with remarkable oxygen tolerance. Combined with photoactivatable Cre recombinase technology, NIR-light stimulation successfully performs genome engineering resulting in the formation of dendritic-spine-like structures of hippocampal neurons.*

Introduction

Optogenetics is a technology allowing light-responsive proteins to regulate cellular events and has contributed to the progress of neuroscience.[1] Since visible light does not penetrate effectively through biological tissues, NIR light has more advantages than visible light as a light source for optogenetics in deep tissues. However, the photoactivation of proteins requires much higher energy photons ($\lambda < 500$ nm) than NIR photons ($\lambda > 700$ nm). To overcome this limitation, recent research efforts have demonstrated that photon upconversion (UC), i.e., converting low-energy NIR light into higher-energy visible light, provides an attractive solution.[2] However, the conventional lanthanide nanoparticles diffuse in liquid conditions from loaded positions. Thus, the development of less diffusible and biocompatible UC materials, such as hydrogels, is highly desired for various biological applications.

Organic UC systems based on triplet–triplet annihilation (TTA) are attractive because of their potential to produce various material forms based on appropriate molecular and matrix designs.[3] In the common TTA-UC scheme, sensitized acceptor (emitter) triplets undergo TTA to produce a higher energy singlet that emits upconverted fluorescence (Supporting Information, Figure S1 a). While the NIR ($\lambda > 700$ nm)-to-blue ($\lambda < 500$ nm) UC is desired for optogenetic stimulation, it was difficult to achieve with a TTA-based mechanism due to the energy loss in the course of the intersystem crossing (ISC) from the singlet (S_1) to triplet (T_1) excited state of the donor (sensitizer). To circumvent this energy loss, new triplet sensitization routes with semiconductor nanocrystals or molecules showing singlet-to-triplet (S–T) absorption have been developed.[4] Our group previously utilized the direct S–T absorption derived from the triplet metal-to-ligand charge transfer (^{3}MLCT) transition of osmium complexes in organic solvents (Supporting Information, Figure S1 b).[5] The triplet energy level of a S–T sensitizer ($Os(bptpy)_2^{2+}$) was tuned for a blue emissive acceptor, 2,5,8,11-tetra-*tert*-butylperylene (TTBP), and the $Os(bptpy)_2^{2+}$-TTBP mixed solution showed a NIR-to-blue TTA-UC with a large anti-Stokes shift of 0.97 eV.

So far, there have been no examples of hydrogels showing NIR-to-blue TTA-UC because of the insolubility of the hydrophobic TTA chromophores in an aqueous environment, limited efficiency of the NIR sensitization, and the massive quenching of excited triplets by dissolved molecular oxygen. The clues to solving these issues can be found in recent advances. The dispersion of chromophores in viscous host matrices effectively suppresses oxygen diffusion and enables air-stable TTA-UC.[6] However, the excited-state lifetime of NIR triplet sensitizers, such as inorganic nanocrystals and S–T absorbers, is often too short to allow collision with acceptors for triplet energy transfer (TET) in such viscous matrices.

In this work, we report the first example of optogenetics based on NIR-to-blue TTA-UC hydrogels (Figure 1). It has

[*] Y. Sasaki, Dr. P. Bharmoria, H. Kouno, Prof. N. Yanai, Prof. N. Kimizuka
Department of Chemistry and Biochemistry, Graduate School of Engineering, Center for Molecular Systems (CMS), Kyushu University
744 Moto-oka, Nishi-ku, Fukuoka 819-0395 (Japan)
E-mail: yanai@mail.cstm.kyushu-u.ac.jp
n-kimi@mail.cstm.kyushu-u.ac.jp
Dr. M. Oshikawa, Prof. I. Ajioka
Center for Brain Integration Research (CBIR), Tokyo Medical and Dental University (TMDU)
1-5-45 Yushima, Bunkyo-ku, Tokyo 113–8510 (Japan)
E-mail: iajioka.cbir@tmd.ac.jp
Prof. A. Hayashi-Takagi
Laboratory of Medical Neuroscience, Institute for Molecular and Cellular Regulation, Gunma University
Maebashi-city, Gunma 371-8512 (Japan)
Prof. A. Hayashi-Takagi, Prof. I. Ajioka, Prof. N. Yanai
PRESTO, JST, Honcho 4-1-8, Kawaguchi, Saitama 332-0012 (Japan)
Prof. M. Sato
Graduate School of Arts and Sciences, The University of Tokyo
Komaba, Meguro-ku, Tokyo 153-8902 (Japan)
Supporting information and the ORCID identification number(s) for the author(s) of this article can be found under: https://doi.org/10.1002/anie.201911025.

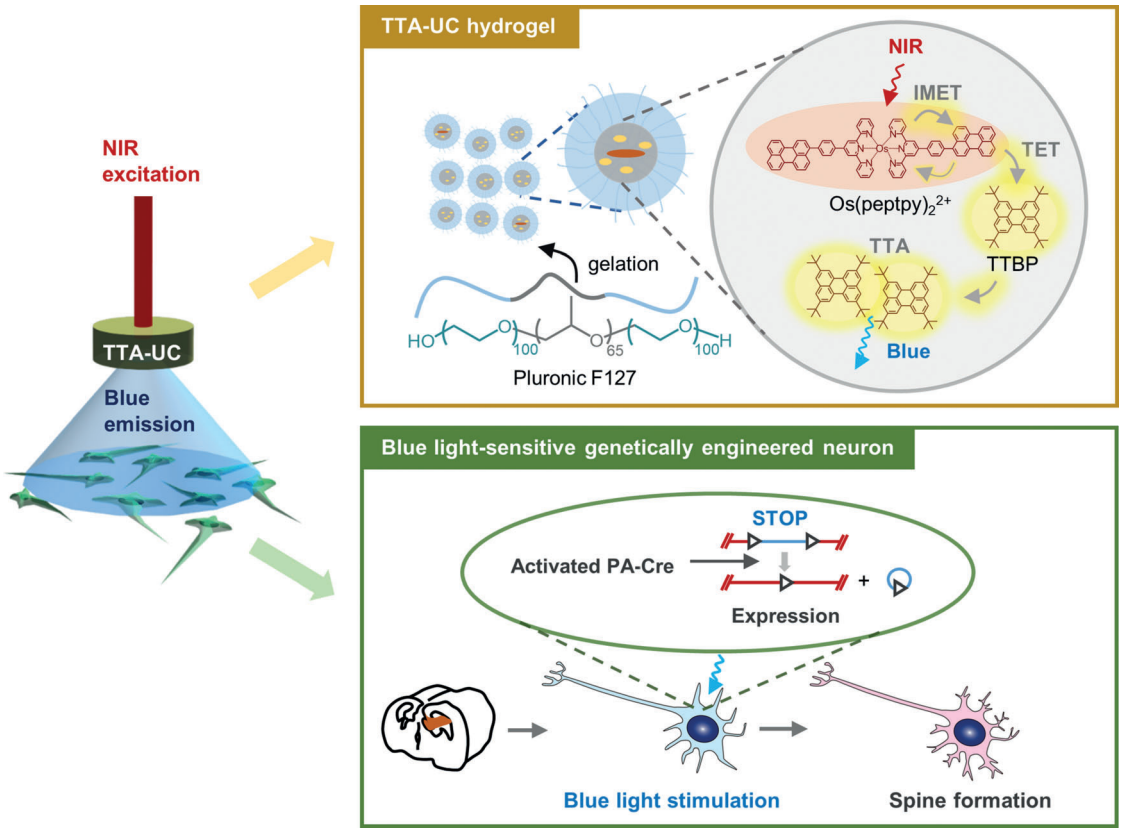

Figure 1. A schematic representation of NIR optogenetics based on TTA-UC hydrogels. A UC hydrogel consisting of Pluronic F127 micelles and UC dyes was irradiated with a continuous-wave NIR laser at 724 nm. The donor $Os(peptpy)_2^{2+}$ absorbed NIR light, and intramolecular energy transfer (IMET) to the triplet pooling phenyl-perylene units elongated the net excited-state lifetime of the sensitizer. After the triplet energy transfer (TET) to acceptor TTBP, bimolecular annihilation (TTA) between TTBP triplets produced a blue upconverted emission. The upconverted blue light induced the activation of blue-light-activatable Cre recombinase (PA-Cre). This activation of PA-Cre resulted in the gene expression important for dendritic-spine formation from genetically engineered hippocampal neurons.

been reported that the triplet lifetime of sensitizers can be elongated by excited-state thermal equilibrium with covalently attached aromatic moieties with long triplet lifetime.[7] We successfully developed the new potential of this strategy to overcome the issue of limited molecular diffusion in viscous oxygen-blocking matrices. Perylene chromophores were covalently attached to Os bisterpyridine complex through phenyl linkages, giving a new complex $Os(peptpy)_2^{2+}$ (Figure 2a). This sensitizer showed a remarkably long phosphorescence lifetime of 23 μs that is long enough for triplet sensitization even in a viscous, biocompatible hydrogel formed from Pluronic F127. Furthermore, an annealing process improves the oxygen-blocking property of the Pluronic F127 hydrogel and enables air-stable NIR ($\lambda > 700$ nm)-to-blue ($\lambda < 500$ nm) UC emission. This could be a simple and powerful method to realize air-stable photochemistry in biocompatible soft materials. This air-stable upconverting hydrogel was used for optogenetic genome engineering by using blue-light-activatable Cre-recombinase (PA-Cre).[8] The employed PA-Cre was recently engineered from a flavin-binding fungal photoreceptor. The reassembly of two split Cre fragments, positive Magnet (pMag) and negative Magnet (nMag), is driven by blue-light irradiation. Under NIR-light illumination, upconverted blue light successfully activated PA-Cre and lead to the morphological regulation of hippocampal neurons, which is important for learning and long-term memory.

Results and Discussion

Elongated photoluminescence lifetimes have been observed for metal complexes and quantum dots modified with chromophoric groups that have a slightly lower triplet energy level than the parent materials.[7] In those works, the lifetime extension is explained by intramolecular energy transfer (IMET) processes and succeeding excited-state equilibration. The equilibrium constant K_{eq} for these processes is estimated by the following relationship:

$$\Delta E \approx -R\,T\ln(K_{eq}) \quad (1)$$

$$K_{eq} = k_{IMET}/k_{bIMET} = \alpha_P/(1-\alpha_P) \quad (2)$$

where k_{IMET} and k_{bIMET} represent the rate constants of IMET and back IMET, respectively, and α_P corresponds to the fraction of excited triplet pooling units. It is important to combine appropriate sensitizer and acceptor units to achieve

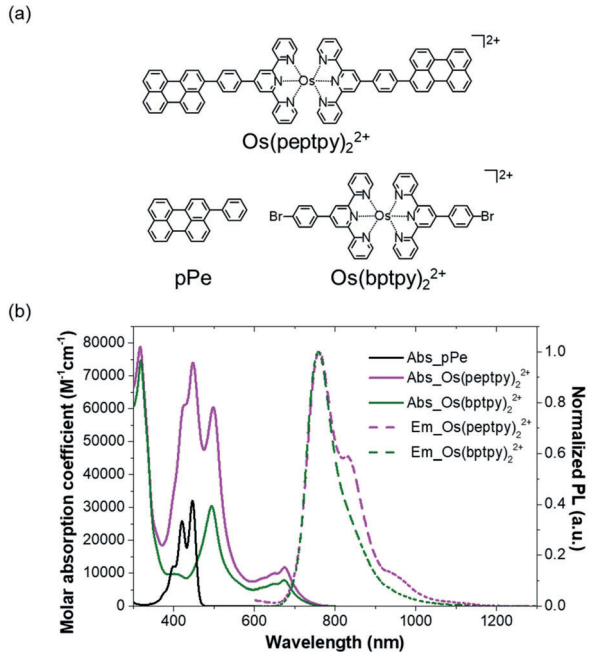

Figure 2. a) Chemical structures of pPe, $Os(bptpy)_2^{2+}$, and $Os(peptpy)_2^{2+}$. b) Absorption spectra of pPe (black), $Os(bptpy)_2^{2+}$, (green) and $Os(peptpy)_2^{2+}$ (magenta) and photoluminescence (PL) spectra of $Os(bptpy)_2^{2+}$ ($\lambda_{ex}=494$ nm, 20 μM) and $Os(peptpy)_2^{2+}$ ($\lambda_{ex}=498$ nm, 20 μM) in deaerated DMF.

efficient IMET with small energy loss. As a suitable acceptor counterpart for donor osmium(II) bis(4′-phenyl-2,2′:6′,2″-terpyridine) ($Os(ptpy)_2$) unit ($T_1=1.63$ eV), we employed phenyl-perylene (pPe) unit ($T_1\approx1.50$ eV based on TD-DFT calculation) which gives small ΔE of −0.13 eV for a high IMET efficiency ($\alpha_P>99\,\%$). Furthermore, we introduced two pPe units to the $Os(ptpy)_2$ unit to enhance the IMET process.[7b,d]

We carried out a series of photophysical characterizations of the donor–acceptor conjugate $Os(peptpy)_2^{2+}$ and compared the results with those of only acceptor pPe and donor $Os(bptpy)_2^{2+}$ (Figure 2a) in deaerated DMF. The solutions were prepared in an Ar-filled glove box (oxygen concentration <0.1 ppm). Absorption peak positions of $Os(peptpy)_2^{2+}$ were almost the same as those of $Os(bptpy)_2^{2+}$ and pPe (Figure 2b). This indicates weak electronic couplings between $Os(ptpy)_2$ unit and pPe units, which is also supported by DFT calculations (Supporting Information, Figure S2). The phenyl ring is twisted against both terpyridine and perylene, which avoids the orbital overlap between these units. A phosphorescence spectrum of $Os(peptpy)_2^{2+}$ in DMF shows a peak at 760 nm, which was almost the same as $Os(bptpy)_2^{2+}$ ($\lambda_{em}=$ 758 nm). It is thus likely that the ^{3}MLCT energy level did not change with the perylene conjugation. The perylene modification caused additional shoulder peaks at around 835 and 950 nm. To understand these new peaks, a phosphorescence spectrum of non-conjugated Os complex $Os(bptpy)_2^{2+}$ was measured at −196 °C (Supporting Information, Figure S3). While the phosphorescence peak at 760 nm almost disappeared, the emission peaks at around 835 and 950 nm remained after freezing. Based on our TD-DFT calculation, the peak at 835 nm (1.49 eV) can be attributed to the emission mainly from the triplet state of the pPe unit.

Importantly, the phosphorescence lifetime of $Os(peptpy)_2^{2+}$ was much longer (24 μs) than that of $Os(bptpy)_2^{2+}$ (0.2 μs) in deaerated DMF at room temperature (Figure 3a).

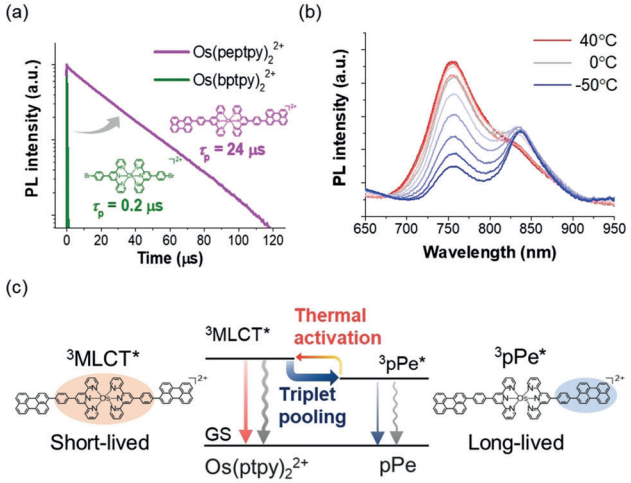

Figure 3. a) Phosphorescence decays of $Os(peptpy)_2^{2+}$ (magenta, $\lambda_{ex}=498$ nm, $\lambda_{em}=743$ nm, 20 μM) and $Os(bptpy)_2^{2+}$ (green, $\lambda_{ex}=494$ nm, $\lambda_{em}=743$ nm, 20 μM) in deaerated DMF. b) Temperature-dependent PL spectra of $Os(peptpy)_2^{2+}$ ($\lambda_{ex}=532$ nm). c) The mechanism of the triplet-lifetime extension and thermally activated delayed phosphorescence of $Os(peptpy)_2^{2+}$.

While the biggest drawback of the S–T absorption sensitizers compared with conventional triplet sensitizers has been the short triplet lifetime, which is disadvantageous for TET to acceptors, the observed triplet lifetime of $Os(peptpy)_2^{2+}$ is comparable to that of benchmark porphyrin-based (ex. $\tau_p\approx42$ μs for platinum(II) tetraphenyltetrabenzoporphyrin)[9] and phthalocyanine-based sensitizers (ex. $\tau_p\approx3.5$ μs for palladium(II) 1,4,8,11,15,18,22,25-octabutoxyphthalocyanine).[10]

Thermal equilibrium among the excited states in $Os(peptpy)_2^{2+}$ was confirmed by measuring its temperature-dependent photoluminescence (PL) spectra (Figure 3b) and time-dependent PL spectra (Supporting Information, Figure S4). By decreasing the temperature from 40 °C to −50 °C, the peak at 835 nm remained, while the peak around 760 nm became weaker. By further decreasing the temperature to −196 °C, the peak around 760 nm almost disappeared (Supporting Information, Figure S3). In the time-dependent PL spectra at room temperature, the spectral shape did not change over the whole lifetime (Supporting Information, Figure S4a,b), and similar decay profiles were observed at 760 nm and 835 nm (Supporting Information, Figure S4c). From these results, we conclude that the extension of the triplet lifetime is based on the excited-state thermal equilibrium between the short-lived ^{3}MLCT state of $Os(ptpy)_2$ and the long-lived triplet state of the conjugated perylene moieties (Figure 3c). In other words, $Os(peptpy)_2^{2+}$ shows thermally activated delayed phosphorescence.

The TTA-UC efficiency of $Os(peptpy)_2^{2+}$-TTBP in DMF ($[Os(peptpy)_2^{2+}]=20$ μM, $[TTBP]=20$ mM) was compared

with that of $Os(bptpy)_2^{2+}$-TTBP ($[Os(bptpy)_2^{2+}] = 20\ \mu M$, $[TTBP] = 20\ mM$) under inert condition (Figure 4a). With excitation at 724 nm, both solutions showed blue UC emission at 484 nm from TTBP (Figure 4b). The emission peak at

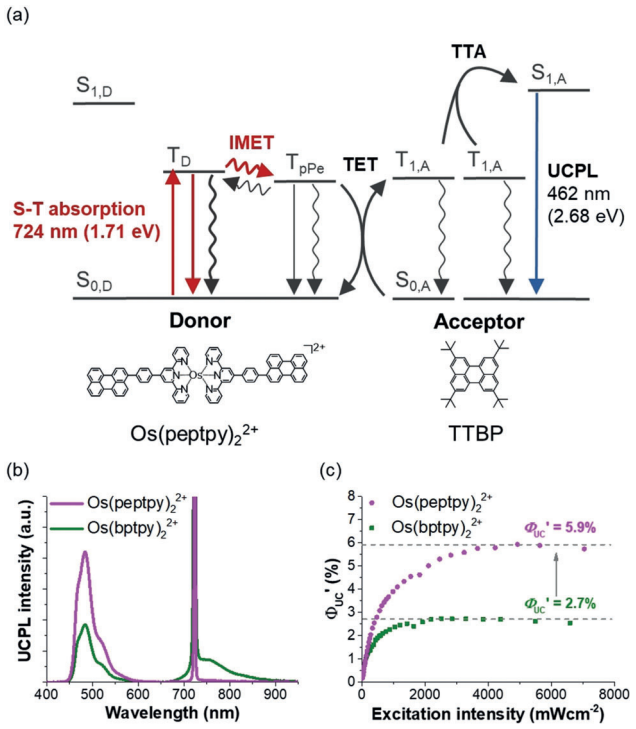

Figure 4. a) Energy diagram of TTA-UC based on S–T absorption and triplet pooling. b) UC emission spectra of $Os(peptpy)_2^{2+}$-TTBP (magenta) and $Os(bptpy)_2^{2+}$-TTBP (green) DMF solution ($\lambda_{ex} = 724$ nm, $I_{ex} = 7.6\ W cm^{-2}$). c) UC quantum efficiency as a function of excitation intensity.

462 nm was partially suppressed mainly due to the self-absorption of TTBP (Supporting Information, Figure S5). The phosphorescence detected for $Os(bptpy)_2^{2+}$-TTBP almost disappeared for $Os(peptpy)_2^{2+}$-TTBP. Therefore, we conclude both Φ_{TET} and Φ_{IMET} are almost 100% for $Os(peptpy)_2^{2+}$-TTBP, which is doubled compared with Φ_{TET} for $Os(bptpy)_2^{2+}$-TTBP (47%).[5] Whereas the energy transfer from pPe ($T_1 \approx 1.49$ eV) to TTBP ($T_1 \approx 1.53$ eV) is endothermic, the much higher concentration of acceptor TTBP makes this small up-hill process entropically favorable.[11] Since Φ_{UC}' is proportional to Φ_{TET}, Φ_{UC}' also increased by a factor of two from 2.7% to 5.9% (Figure 4c and Supporting Information, Table S1). A further improvement would be expected by suppressing the reabsorption of upconverted emission by the sensitizer.

Notably, the elongated excited-state lifetime of the S–T sensitizer $Os(peptpy)_2^{2+}$ enabled TET to TTBP even in the viscous micelle cores. We fabricated hydrogels composed of donor $Os(peptpy)_2^{2+}$, acceptor TTBP, and Pluronic F127 ($[Os(peptpy)_2^{2+}] = 15\ nmol\ g^{-1}$, $[TTBP] = 7.5\ \mu mol\ g^{-1}$, [Pluronic F127] $= 24\ \mu mol\ g^{-1}$, Supporting Information, Figure S7). These components were first dissolved in DMF, and DMF was removed under vacuum at 100 °C. The remaining solid was mixed with water at 0 °C, and $Os(peptpy)_2^{2+}$-TTBP-Pluronic hydrogels were produced by subsequent annealing at 80 °C. The control $Os(bptpy)_2^{2+}$-TTBP-Pluronic hydrogel showed almost no UC emission under excitation by a 724 nm laser. On the other hand, a blue UC emission was observed from $Os(peptpy)_2^{2+}$-TTBP-Pluronic hydrogel (Figure 5a). The UC emission could be observed at relatively low excitation intensity of $I_{ex} = 5\ W cm^{-2}$ (Supporting Information, Figure S8a). The UC emission spectrum overlapped well with a blue LED light source spectrum which is used for conventional optogenetics (Supporting Information, Figure S8b).

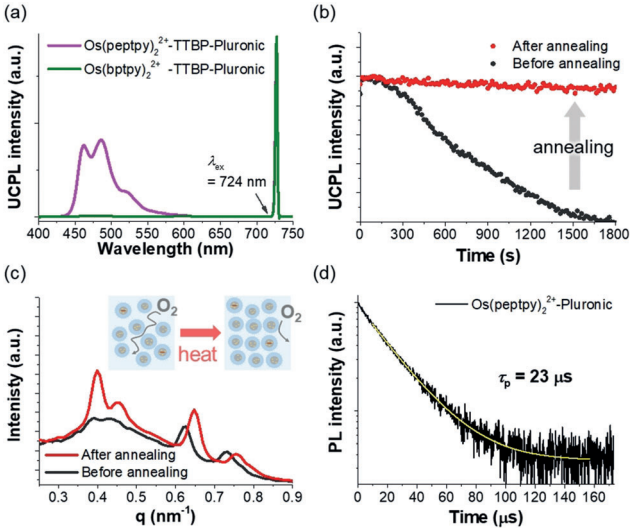

Figure 5. a) UC emission spectra of the air-saturated $Os(peptpy)_2^{2+}$-TTBP-Pluronic hydrogel (magenta) and $Os(bptpy)_2^{2+}$-TTBP-Pluronic hydrogel (green) after annealing at 80 °C ($I_{ex} = 78\ W cm^{-2}$, $\lambda_{ex} = 724$ nm, 610 nm short pass filter). b) Time-dependent UC emission intensity ($I_{ex} = 30\ W cm^{-2}$) of the air-saturated $Os(peptpy)_2^{2+}$-TTBP-Pluronic hydrogel before (black) and after (red) annealing at 80 °C. c) SAXS profiles of the air-saturated $Os(peptpy)_2^{2+}$-TTBP-Pluronic hydrogel before (black) and after (red) annealing at 80 °C. d) Phosphorescence decays of $Os(peptpy)_2^{2+}$-Pluronic hydrogel ($\lambda_{ex} = 498$ nm, $\lambda_{em} = 760$ nm, 20 μM) after annealing at 80 °C.

Interestingly, we found that the air stability of the UC emission can be improved by annealing the hydrogels at 80 °C (Figure 5b). Since the excited triplets are easily quenched by molecular oxygen under air-saturated conditions, it is apparent that the oxygen diffusion was suppressed by the heat treatment. Without annealing, the UC emission of the $Os(peptpy)_2^{2+}$-TTBP-Pluronic hydrogel almost disappeared within 30 minutes under continuous NIR irradiation. In stark contrast, the annealed UC gel retained more than 90% of UC emission intensity after 30 minutes of NIR irradiation. To get some insight into this drastic annealing effect, small angle X-ray scattering (SAXS) measurements were carried out for $Os(peptpy)_2^{2+}$-TTBP-Pluronic hydrogels before and after the annealing. It has been reported that 30 wt% Pluronic F127-based hydrogels show SAXS peaks at 0.39 and 0.45 nm^{-1}, which become stronger after heat treatment and have been assigned to the micelle assemblies with fcc order.[12] Both of the $Os(peptpy)_2^{2+}$-TTBP-Pluronic hydrogels without/with

annealing showed peaks at similar positions around 0.40 and 0.45 nm^{-1}, but the peak intensity was largely increased by the annealing process (Figure 5c). It indicates the improved packing order of micelles resulting from annealing, which would reduce the oxygen diffusivity and consequently enhance the air stability of the UC emission. Since the TTA-UC in nonionic surfactant micelles dispersed in aqueous solution usually requires deaerated conditions,[13] the observed air-stability improvement of the Pluronic hydrogels is noteworthy for biological applications.

The TET efficiency from $Os(peptpy)_2^{2+}$ to TTBP was estimated based on the phosphorescence lifetime in Pluronic hydrogel. Without TTBP, the perylene-conjugated $Os(peptpy)_2^{2+}$ showed a phosphorescence lifetime of 23 μs (Figure 5d). The addition of TTBP shortened the lifetime of $Os(peptpy)_2^{2+}$ to 6.7 μs (Supporting Information, Figure S8c), which gave a Φ_{TET} ($=1-\tau_p/\tau_{p,0}$) of 71%. The occurrence of triplet back energy transfer from TTBP to $Os(peptpy)_2^{2+}$ was also suggested by the long phosphorescence decay component of 128 μs. The fact that the UC emission disappeared at −196 °C indicates that the TET process operates via molecular diffusion and collision rather than the energy migration in dye aggregates (Supporting Information, Figure S8d).

The TTA-based UC mechanism was supported by the excitation intensity dependence of the UC emission. A double logarithmic plot for the UC emission intensity of the $Os(peptpy)_2^{2+}$-TTBP-Pluronic hydrogel showed a quadratic-to-linear transition with threshold excitation intensity I_{th} of 13 $W cm^{-2}$ (Supporting Information, Figure S8e). The absolute quantum efficiency of this hydrogel was relatively low (<0.1%). The UC emission intensity was not improved by deaeration of hydrogels by freeze-pump-thaw cycles, suggesting the minor effect of dissolved oxygen on the UC efficiency. While the reduction of excitation intensity and the improvement of UC efficiency by enhanced energy migration in controlled molecular assemblies remain as important future works,[14] the current TTA-UC properties were found to be enough to demonstrate the proof-of-concept of NIR optogenetics as shown below.

To apply this upconverting hydrogel for optogenetic genome engineering, we used a PA-Cre system (Supporting Information, Figure S9a).[8] We used Cre-reporter GFP (Supporting Information, Figure S9b) and transfection-reporter mCherry (Supporting Information, Figure S9c) to visualize optogenetic manipulation. Cre-reporter GFP starts to be expressed in the presence of activated PA-Cre, while it is not expressed in the absence of activated PA-Cre because of a polyA signal sequence between two loxP sites. The cerebral cortex was dissected from a day (E) 13 embryo and pCAG-PA-Cre, pCALNL-GFP, and pCAG-mCherry plasmids were transfected into cortical cells by electroporation[15] (Supporting Information, Figure S9d). After 48 hours in culture, transfected cortical neurons were illuminated as described in the Supporting Information. The total number of cortical cells, counted after removing dead cells, was not significantly affected by the NIR-light illumination in the presence of the UC hydrogel (Supporting Information, Figure S10), suggesting that the UC hydrogel did not affect cell viability in this experiment. NIR-light stimulation with the UC hydrogel

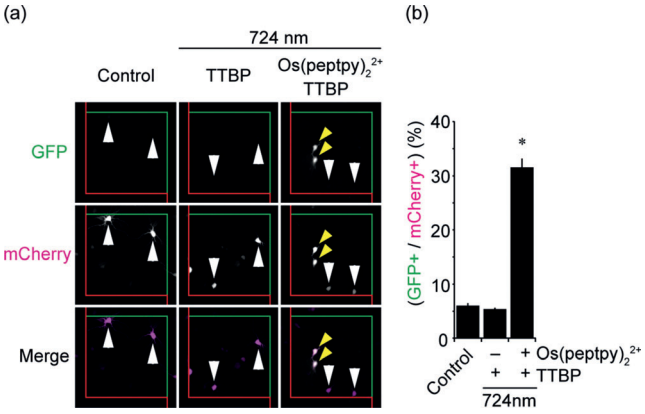

Figure 6. a) Fluorescence microscopy images of GFP only (white), mCherry only (white), and an overlay of GFP (green) and mCherry (magenta). Arrowheads indicate GFP and mCherry double-positive cells. Arrows indicate mCherry single-positive cells. Grid represents the counting frame (200×200 μm) for stereological analysis. b) Cell scoring of GFP-positive cells among mCherry-positive cells. * $p<0.05$ (compared to values for control).

increased the ratio of GFP-positive cells, while NIR-light stimulation with the TTBP hydrogel did not (Figure 6a,b), indicating that the UC hydrogel works as a tool for NIR UC optogenetics.

Using the UC hydrogel, we examined whether NIR light stimulation regulates hippocampal dendritic spines involved in learning and long-term memory by receiving excitatory input from axons.[16] Rac1(Q61L), the constitutive active form of Rac1,[17] is known to promote dendritic spine formation.[18] We used Cre-reporter Rac1(Q61L) to promote hippocampal dendritic spine formation (Supporting Information, Figure S11a). The hippocampus was dissected from E15 embryo and pCAG-PA-Cre, pCALNL-Rac1(Q61L), pCALNL-GFP, and pCAG-mCherry plasmids were transfected into hippocampal cells (Supporting Information, Figure S11b). At 10 hours after NIR-light stimulation with the UC hydrogel, both GFP expression and the formation of dendritic-spine-like structures were observed (Figure 7e–h). On the other hand, the non-light stimulation condition did not show GFP expression or the formation of dendritic-spine-like structures (Figure 7a–d). To examine the dynamics of spine-like formation, we performed time-lapse imaging analysis (Supporting Information, Figure S11b). Newly generated dendritic protrusions were observed by NIR-light stimulation with the UC hydrogel from 6 hours after stimulation but not with the control (Figure 7i,j and Supporting Information, Movie S1), suggesting that the NIR-light stimulation promoted the formation of dendritic-spine-like structures. From these results, the NIR-light stimulation with the TTA-UC hydrogel regulates neuronal morphology, which is important for learning and long-term memory.

Conclusion

We demonstrate NIR optogenetics by NIR-to-blue TTA-UC for the first time. The stable TTA-UC emission in the

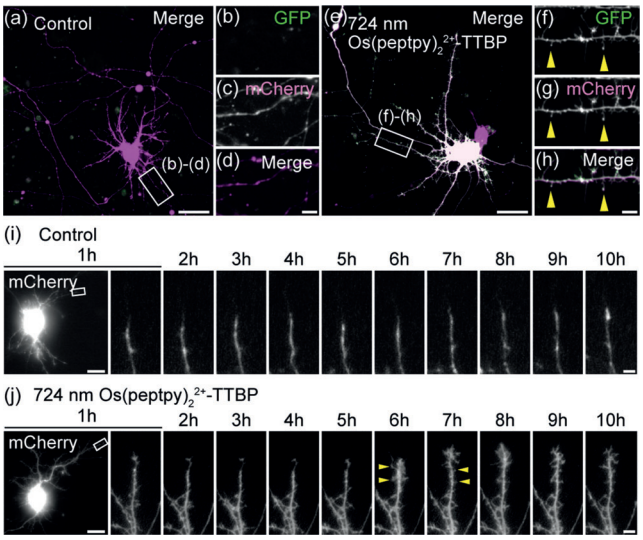

Figure 7. a–h) Fluorescence microscopy images of GFP only (white) (b,f), mCherry only (white) (c,g), and an overlay of GFP (green) and mCherry (magenta) (a,d,e,h). Arrowheads indicate dendritic-spine-like structures. Scale bars: 20 μm (a,e) and 5 μm (b–d, f–h). i,j) Time-lapse imaging of hippocampal neurons. Arrowheads indicate the formation of dendritic-spine-like structures. Scale bars: 20 μm (left column) and 5 μm (others).

hydrogel is achieved by the combination of two concepts. First, the elongated triplet lifetime of the S–T sensitizer by excited-state thermal equilibrium with long-lived energy-pooling perylene units allows the triplet energy transfer to acceptor molecules even in the viscous hydrogels. Second, although the triplet excited state is usually quenched by dissolved oxygen molecules, the heat treatment of Pluronic hydrogels induces micelle rearrangement to form more ordered structures, endowing the UC hydrogels with an oxygen-blocking property. This simple method to protect oxygen-sensitive species with a biocompatible, widely used polymer would be of great interest for many biological applications. We prove that the NIR-to-blue TTA-UC hydrogels work as a tool for NIR optogenetics. The blue UC emission activates PA-Cre, resulting in the expression of Cre-reporter GFP in cortical neurons and the Cre-reporter constitutively active Rac1, which promotes the formation of hippocampal spine-like structure. Given the possible potential of TTA-UC to offer a variety of soft materials, TTA-UC-based NIR optogenetics is one of the ideal tools for deep tissue treatment. This study could open a new era of in vivo NIR photochemistry utilizing TTA-UC emission as an internal light source for optogenetics in deep tissues.

Acknowledgements

This work was partly supported by JSPS KAKENHI grant number JP25220805, JP17H04799, JP16H06513, JP16H00844, PRESTO program on "Molecular Technology and Creation of New Functions" from JST (JPMJPR14KE, JPMJPR14K1), the Izumi Science and Technology Foundation, and the Asahi Glass Foundation. P.B. acknowledges JSPS postdoctoral fellowships for foreign researchers.

Conflict of interest

The authors declare no conflict of interest.

Keywords: near-infrared light · genome engineering · photon upconversion · singlet-to-triplet absorption · triplet–triplet annihilation

[1] C. K. Kim, A. Adhikari, K. Deisseroth, *Nat. Rev. Neurosci.* **2017**, *18*, 222 – 235.
[2] J. Zhou, Q. Liu, W. Feng, Y. Sun, F. Li, *Chem. Rev.* **2015**, *115*, 395 – 465.
[3] a) S. Baluschev, T. Miteva, V. Yakutkin, G. Nelles, A. Yasuda, G. Wegner, *Phys. Rev. Lett.* **2006**, *97*, 143903; b) T. N. Singh-Rachford, F. N. Castellano, *Coord. Chem. Rev.* **2010**, *254*, 2560 – 2573; c) J. Zhao, S. Ji, H. Guo, *RSC Adv.* **2011**, *1*, 937 – 950; d) Y. C. Simon, C. Weder, *J. Mater. Chem.* **2012**, *22*, 20817 – 20830; e) A. Monguzzi, R. Tubino, S. Hoseinkhani, M. Campione, F. Meinardi, *Phys. Chem. Chem. Phys.* **2012**, *14*, 4322 – 4332; f) V. Gray, K. Moth-Poulsen, B. Albinsson, M. Abrahamsson, *Coord. Chem. Rev.* **2018**, *362*, 54 – 71; g) J. C. Wang, S. P. Hill, T. Dilbeck, O. O. Ogunsolu, T. Banerjee, K. Hanson, *Chem. Soc. Rev.* **2018**, *47*, 104 – 148.
[4] a) Z. Huang, X. Li, M. Mahboub, K. M. Hanson, V. M. Nichols, H. Le, M. L. Tang, C. J. Bardeen, *Nano Lett.* **2015**, *15*, 5552 – 5557; b) M. Mahboub, Z. Huang, M. L. Tang, *Nano Lett.* **2016**, *16*, 7169 – 7175; c) S. Amemori, Y. Sasaki, N. Yanai, N. Kimizuka, *J. Am. Chem. Soc.* **2016**, *138*, 8702 – 8705.
[5] Y. Sasaki, S. Amemori, H. Kouno, N. Yanai, N. Kimizuka, *J. Mater. Chem. C* **2017**, *5*, 5063 – 5067.
[6] a) J.-H. Kim, F. Deng, F. N. Castellano, J.-H. Kim, *Chem. Mater.* **2012**, *24*, 2250 – 2252; b) D. C. Thévenaz, A. Monguzzi, D. Vanhecke, R. Vadrucci, F. Meinardi, Y. C. Simon, C. Weder, *Mater. Horiz.* **2016**, *3*, 602 – 607; c) P. Bharmoria, S. Hisamitsu, H. Nagatomi, T. Ogawa, M.-a. Morikawa, N. Yanai, N. Kimizuka, *J. Am. Chem. Soc.* **2018**, *140*, 10848 – 10855; d) C. Ye, J. Ma, S. Chen, J. Ge, W. Yang, Q. Zheng, X. Wang, Z. Liang, Y. Zhou, *J. Phys. Chem. C* **2017**, *121*, 20158 – 20164.
[7] a) W. E. Ford, M. A. J. Rodgers, *J. Phys. Chem.* **1992**, *96*, 2917 – 2920; b) D. S. Tyson, F. N. Castellano, *J. Phys. Chem. A* **1999**, *103*, 10955 – 10960; c) X.-y. Wang, A. Del Guerzo, R. H. Schmehl, *J. Photochem. Photobiol. C* **2004**, *5*, 55 – 77; d) N. D. McClenaghan, Y. Leydet, B. Maubert, M. T. Indelli, S. Campagna, *Coord. Chem. Rev.* **2005**, *249*, 1336 – 1350; e) D. Liu, Y. Zhao, Z. Wang, K. Xu, J. Zhao, *Dalton Trans.* **2018**, *47*, 8619 – 8628; f) Q. Chen, Y. Liu, X. Guo, J. Peng, S. Garakyaraghi, C. M. Papa, F. N. Castellano, D. Zhao, Y. Ma, *J. Phys. Chem. A* **2018**, *122*, 6673 – 6682; g) C. Mongin, P. Moroz, M. Zamkov, F. N. Castellano, *Nat. Chem.* **2018**, *10*, 225 – 230.
[8] F. Kawano, R. Okazaki, M. Yazawa, M. Sato, *Nat. Chem. Biol.* **2016**, *12*, 1059 – 1064.
[9] T. N. Singh-Rachford, F. N. Castellano, *J. Phys. Chem. Lett.* **2010**, *1*, 195 – 200.
[10] T. N. Singh-Rachford, F. N. Castellano, *J. Phys. Chem. A* **2008**, *112*, 3550 – 3556.
[11] Y. Y. Cheng, B. Fückel, T. Khoury, R. G. C. R. Clady, N. J. Ekins-Daukes, M. J. Crossley, T. W. Schmidt, *J. Phys. Chem. A* **2011**, *115*, 1047 – 1053.

[12] N. A. K. Meznarich, K. A. Juggernauth, K. M. Batzli, B. J. Love, *Macromolecules* **2011**, *44*, 7792 – 7798.
[13] A. Turshatov, D. Busko, S. Baluschev, T. Miteva, K. Landfester, *New J. Phys.* **2011**, *13*, 083035.
[14] N. Yanai, N. Kimizuka, *Acc. Chem. Res.* **2017**, *50*, 2487 – 2495.
[15] M. Oshikawa, K. Okada, K. Nakajima, I. Ajioka, *Development* **2013**, *140*, 2310 – 2320.
[16] B. Leuner, J. Falduto, T. J. Shors, *J. Neurosci.* **2003**, *23*, 659 – 665.
[17] N. Lamarche, N. Tapon, L. Stowers, P. D. Burbelo, P. Aspenström, T. Bridges, J. Chant, A. Hall, *Cell* **1996**, *87*, 519 – 529.
[18] L. Luo, T. K. Hensch, L. Ackerman, S. Barbel, L. Y. Jan, Y. N. Jan, *Nature* **1996**, *379*, 837 – 840.

Manuscript received: August 28, 2019
Accepted manuscript online: September 23, 2019
Version of record online: ■■ ■■, ■■■■

Research Articles

Optogenetics

Y. Sasaki, M. Oshikawa, P. Bharmoria, H. Kouno, A. Hayashi-Takagi, M. Sato, I. Ajioka,* N. Yanai,* N. Kimizuka* _____ ▮▮▮▮–▮▮▮▮

Near-Infrared Optogenetic Genome Engineering Based on Photon-Upconversion Hydrogels

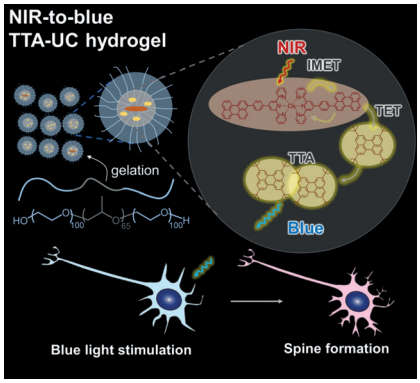

Near-infrared (NIR) light-triggered optogenetics with triplet–triplet annihilation-based photon upconversion (TTA-UC) is demonstrated. Triplet-lifetime extension by the covalent conjugation of donor and acceptor and a heat-induced conformational change of the hydrogel that prevents oxygen diffusion enables the formation of dendritic-spine-like structures by hippocampal neurons, induced by NIR-to-blue TTA-UC.